Volume 54
Number 35
21 September 2025
Pages 12989-13366

Dalton Transactions

An international journal of inorganic chemistry

rsc.li/dalton

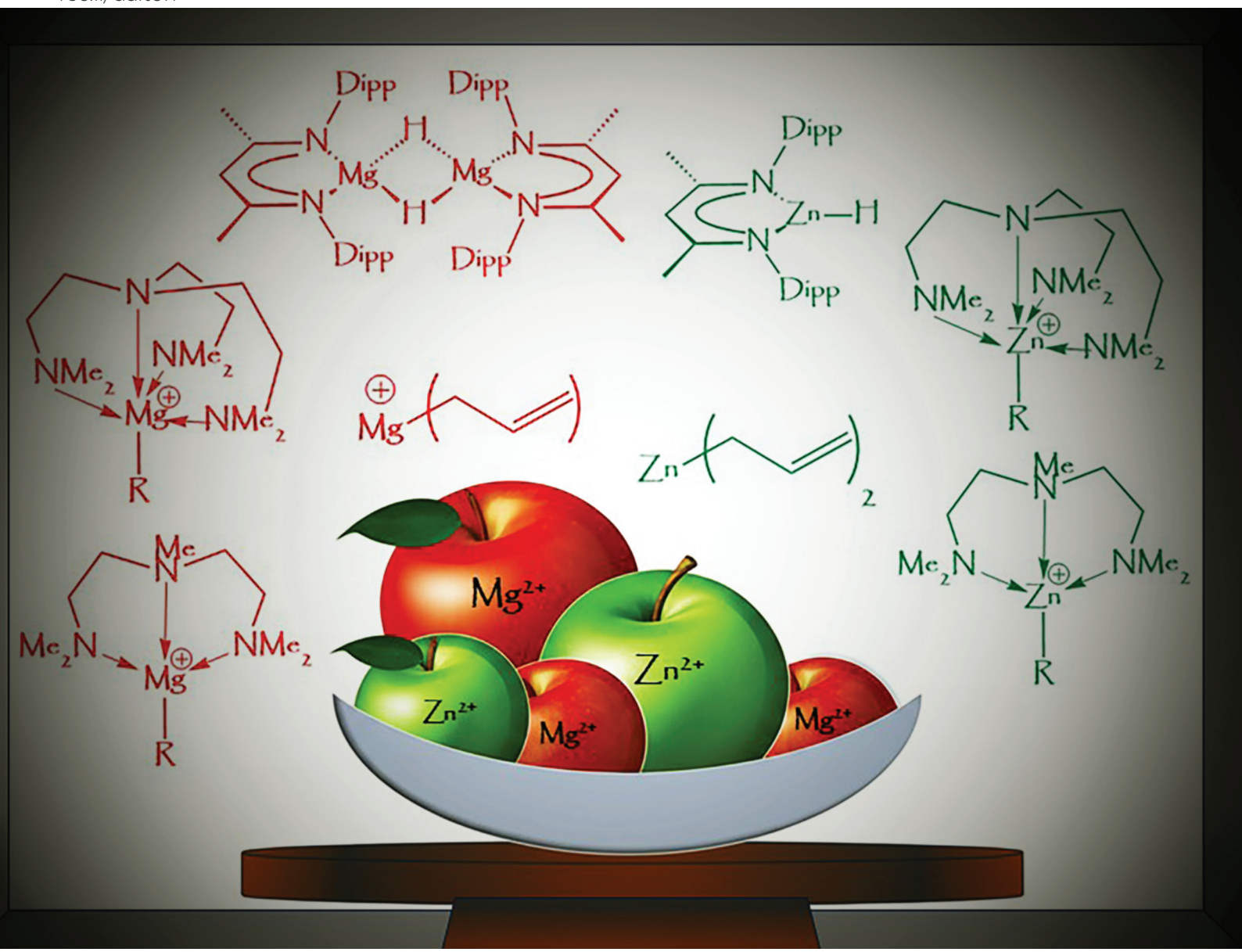

ISSN 1477-9226

ROYAL SOCIETY OF CHEMISTRY

PERSPECTIVE

Ajay Venugopal *et al.*

Isostructural Mg and Zn compounds: analogies and differences in reactivity

Dalton Transactions

ROYAL SOCIETY OF CHEMISTRY

PERSPECTIVE

View Article Online
View Journal | View Issue

Cite this: *Dalton Trans.*, 2025, **54**, 13005

Isostructural Mg and Zn compounds: analogies and differences in reactivity

Kriti Pathak, Suban Kundu, Sheetal Kathayat Bisht and Ajay Venugopal *

In recent years, active efforts to assess similarities and differences in the reactivity of isostructural magnesium and zinc complexes have witnessed reasonable growth. The advancements in their chemistry concerning catalytic reduction of compounds like olefins, imines, nitriles, carbonyls and CO_2, alkene isomerisation as well as hydrogen uptake and release have garnered attention. The unique characteristics of Mg and Zn stem from their similarities at the molecular level but differences in electrophilicity after complexation. This is reflected in the structures and/or chemistry of these isostructural complexes, making their study even more interesting. Consequently, the chemistry of Mg and Zn complexes with suitable co-ligands has seen progression both in terms of synthetic methodology as well as isolation of unique frameworks, ranging from mono- or bimetallic hydride complexes to multimetallic hydride clusters, cationic complexes, amidoboranes as well as σ-complexes with transition metals. The organisation of this review is based on the categories of ligand systems that stabilise these precarious complexes, specifically β-diketiminate and its derivatives, N-heterocyclic carbene motifs, NNNN-macrocyclic motifs, anionic nitrogen donor motifs and allylic donor motifs. The synthesis and structural aspects of these main group complexes are discussed, along with their reactivity, applications, and mechanistic insights into some of the reactions.

Received 25th April 2025,
Accepted 17th July 2025

DOI: 10.1039/d5dt00978b

rsc.li/dalton

1. Introduction

Molecular compounds of magnesium and zinc show significant similarities in their chemical behaviour. For instance, the dications of the two metals are both stable with closed shell configurations (Mg^{2+}: [Ne]$3s^0$; Zn^{2+}: [Ar]$3d^{10}4s^0$) and have comparable ionic radii across a variety of coordination numbers (Table 1).[1]

The coordination geometries of magnesium and zinc are also very similar; there are complexes where these two metals can be substituted.[2–10] In addition, the metal oxides MgO and ZnO and vitriols like $MgSO_4{\cdot}7H_2O$ and $ZnSO_4{\cdot}7H_2O$ exhibit isomorphism in their crystalline forms, permitting unrestricted interchange of magnesium and zinc.[3,4] However, according to the hard and soft acid–base principle, Mg^{2+} is harder than Zn^{2+} primarily because of the electronegativity difference between these two atoms.[11,12] The charge/radius value is significantly different for both ions since the effective nuclear charge of Zn^{2+} is higher than Mg^{2+} due to the presence of low shielding d-electrons in the former. Hence, regardless of the similarities, the Lewis acidity of isostructural molecular magnesium and zinc compounds may differ significantly.[11,12] The inconsistent chemical behaviour of certain isostructural compounds, such as organozinc and organomagnesium compounds, in terms of reactivity and catalysis, does frequently reflect this. To illustrate, magnesium–carbon bonds are significantly more polar than zinc–carbon bonds.[13] This difference in polarity has implications in several reactions involving the addition of Mg–C and Zn–C across unsaturated organic substrates.[13] Moreover, organomagnesium reagents are stronger nucleophiles than organozinc reagents. Hence, they have generally found preference in synthetic applications, even though organozinc reagents were among the earliest identified organometallic compounds.[14–16] Nevertheless, there is a renewed focus on zinc reagents due to a growing appreciation for their typical properties, which include mild nucleophilicity

Table 1 Ionic radii of Mg^{2+} and Zn^{2+} ions with different coordination numbers

	Ionic radii (Å)	
Coordination number	Mg^{2+}	Zn^{2+}
4	0.57	0.60
5	0.66	0.68
6	0.72	0.74
8	0.89	0.90

School of Chemistry, Indian Institute of Science Education and Research Thiruvananthapuram, Vithura, Thiruvananthapuram 695551, India.
E-mail: venugopal@iisertvm.ac.in

combined with good functional group tolerance, making them more chemoselective and stereospecific than organomagnesium reagents.[17–19] Furthermore, several molecular zinc complexes have become more significant as highly active and selective catalysts relative to their magnesium counterparts for a wide range of transformations in addition to their stoichiometric uses.[17–20]

There are detailed reviews dedicated to the synthetic and structural facets of molecular magnesium and zinc complexes, along with certain areas of their chemistry.[21–23] However, to the best of our knowledge, there is no comprehensive account that focuses on the analogous and/or contradictory chemical behaviours of these complexes. In this perspective article, we provide an overview of the analogies and highlight the differences between isostructural magnesium and zinc complexes. Hydride archetypes are mainly prominent in this review as they showcase rich and diverse chemistry. Other archetypes, such as cationic and amidoborane complexes, are also discussed. The ligand systems that have been used to stabilise these precarious main group complexes are the basis for the organisation of this article; these systems include mainly nitrogen and carbon donor ligands: (i) the β-diketiminate ligand and its derivatives, (ii) N-heterocyclic carbenes as ligands, (iii) NNNN-macrocyclic ligands, (iv) anionic nitrogen donor-based ligands and (v) allyl anions as ligands. It is by no means intended to diminish the importance of the other archetypes of magnesium and zinc complexes like the alkyl and low oxidation state complexes, but neither is it to give a comprehensive account for each prototype.

2. β-Diketiminate (BDI or 'nacnac') ligands

Modern coordination and organometallic chemistry have extensively utilised the monoanionic β-diketiminate (BDI or 'nacnac') ligands[24–26] $[(ArNCR)_2CH]^-$ ($^{R}BDI^{Ar}$; Ar = aryl substituents, R = alkyl substituents), due to their ease of synthetic accessibility combined with steric and electronic tunability.[27,28] These ligands have been used extensively throughout the periodic table and have been essential in isolating highly reactive species and intermediates.[29] Numerous examples of magnesium hydrides supported by the BDI ligands of varying steric bulk have been reported to date.[21] One of the approaches for their synthesis involves the reaction of a parent metal alkyl with a hydrosilane, resulting in the formation of the desired hydride *via* σ-bond metathesis.[30] For example, dimeric magnesium hydrides $[(^{R}BDI^{Dipp})Mg(\mu\text{-}H)_2]$ (**1a** and **1b**) (Dipp = 2,6-iPr_2-C_6H_3; R = Me (**1a**), *t*Bu (**1b**)) were obtained in 40% yields from the reaction of phenylsilane with the corresponding magnesium alkyls (Scheme 1).[30] **1a** can also be obtained *via* an alternative route that involves pyrolysing the aminoborane $[(^{Me}BDI^{Dipp})MgNH(iPr)BH_3]$ in benzene.[31] This reaction proceeds *via* β-hydride elimination and affords **1a** in a significantly higher yield (89%), alongside a borazine by-product $[(iPrNBH)_3]$ (Scheme 1).[31]

In contrast to the magnesium hydrides **1a** and **1b**, BDI-supported zinc hydrides are stable in both dimeric and monomeric forms and may simply be synthesized by reacting the corresponding zinc halides with hydride sources like NaH, CaH_2 or $KNH(iPr)BH_3$.[32,33] For example, the dimeric zinc hydride $[\{(^{Me}BDI^{Mes})ZnH\}_2]$ (**2**: Mes = 2,4,6-$Me_3C_6H_2$) was synthesized by reacting the corresponding BDI-supported zinc halides $[(^{Me}BDI^{Mes})ZnX]$ (X = Cl or I) with NaH or $KNH(iPr)BH_3$ (Scheme 1).[31] The monomeric zinc hydride $[(^{Me}BDI^{Dipp})ZnH]$ (**3**) was obtained by using a sterically more demanding N-bound aryl group (Dipp; Scheme 1).[33] In contrast, the rare monomeric magnesium hydride $[(^{tBu}BDI^{Dipp})MgH(DMAP)]$ (**4**) could only be accessed by allowing complexation of the significantly basic *N*,*N*-dimethylpyridin-4-amine (DMAP) with compound **1b** having a much bulkier $^{tBu}BDI^{Dipp}$ ligand.[34] A summary of some interesting reactivities of these hydrides is provided below.

Catalytic hydrosilylation of alkenes *vs.* nitriles

The hydridomagnesiation of less reactive and functionalized alkenes has consistently been an appealing yet challenging route towards the formation of Mg–C bond(s).[35] The reasons being (i) the lack of alternative general synthetic approaches for Mg–C bond formation, which almost exclusively depends on the 'direct reaction' of elemental magnesium with an organohalide, and (ii) the disadvantageous occurrence and use of residual halides and ether solvents, respectively, in the existing methods.[35,36] Notwithstanding this, the reactivity of dimeric β-diketiminato magnesium hydride $[(^{Me}BDI^{Dipp})Mg(\mu\text{-}H)_2]$ (**1a**) towards terminal alkenes afforded the corresponding organomagnesium derivatives.[35] For example, the reaction of **1a** with terminal alkenes like 1-hexene proceeds at 80 °C, yielding consistent alkylmagnesium organometallics, *viz.*, *n*-hexyl. Additionally, it was noted that the steric demands of the alkene reagent greatly dictate the ease and regioselectivity of these reactions.[35] For instance, reactions with terminal alkenes like 1,1-diphenylethene or styrene proceed at relatively high temperatures of ~100 °C, with the former alkene yielding the magnesium 1,1-diphenylethyl derivative as the single reaction product, while the reaction with styrene afforded a mixture of 2-phenylethyl and 1-phenylethyl products.[35] In addition, **1a** was found to be unreactive towards internal alkenes other than the strained bicyclic alkene norbornene.[35]

This Mg–H/C=C insertion reactivity lays the foundation for the catalytic hydrosilylation of terminal alkenes with $PhSiH_3$.[35]

The reaction is slow, and performing it at relatively high temperatures reduces the time frame. Regardless, the reaction undergoes complete conversion in either case, with a selective preference for the anti-Markovnikov organosilane product.[35] For instance, the reaction between 1-hexene and $PhSiH_3$ in the presence of **1a** leads to complete conversion to *n*-hexyl(phenyl) silane. This preference for the anti-Markovnikov organosilane product fits with (i) the high regioselectivity of the stoichiometric insertion reaction to afford the terminal *n*-hexylmagnesium product and (ii) the sequential proceeding of Mg–H/C=C insertion with Mg–C/Si–H metathesis being the

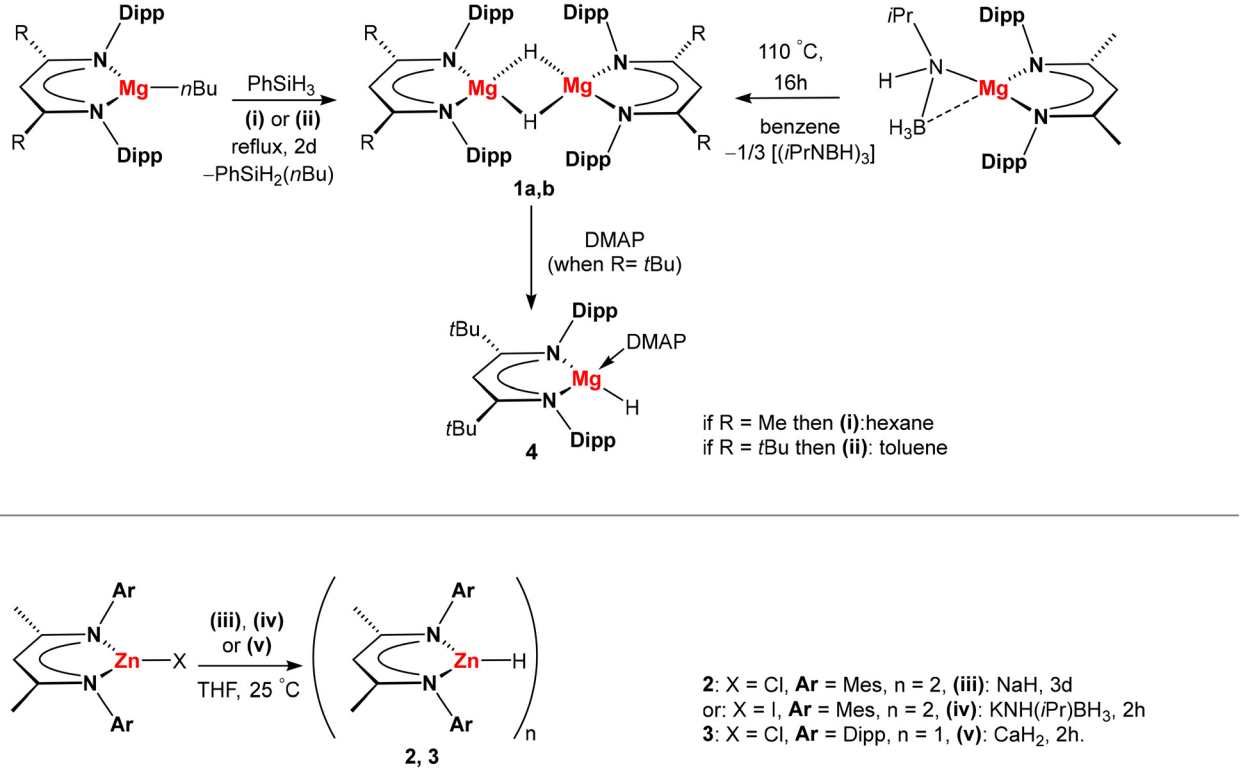

Scheme 1 Synthesis of BDI-stabilised magnesium and zinc hydrides. Top: synthesis of dimeric magnesium hydrides **1a** (R = Me) by hydrosilane metathesis as well as β-hydride elimination routes, with **1b** (R = *t*Bu) and the monomeric magnesium hydride (**4**) as a DMAP adduct. Bottom: synthesis of dimeric and monomeric zinc hydrides **2** and **3**.

operational mechanism of the reaction, as demonstrated in Scheme 2.[35]

The related monomeric zinc hydride [(^{Me}BDI^{Dipp})ZnH] (**3**), on the other hand, was found to have an unexpected role in the chemoselective hydrosilylation of nitriles under mild conditions.[37] The catalytic role of **3** in the chemoselective monoreduction of nitriles to synthetically valuable *N*-silylimines is the first example of such catalysis in the absence of a transition metal.[37] For example, benzonitrile undergoes rapid reduction by $PhSiH_3$ in the presence of **3** to the *N*-silylimine PhCH = $NSiH_2Ph$ at room temperature. Mechanistic studies rationalize the basis of chemoselectivity in the hydrosilylation of nitriles to *N*-silylimines by proposing a novel hydride mechanism, as illustrated in Scheme 2. This involves activation of the silane by the Lewis acidic zinc hydride catalyst **3**, followed by an outer sphere transfer of the zinc hydride to the nitrile substrate *via* a concerted 6-membered cyclic transition state (see ref. 36 for the significance of the reaction constants k_1, k_{-1} and k_2 mentioned in Scheme 2).[37]

Reactions with copper(I) arene complexes: Mg *vs.* Zn

The magnesium and zinc hydrides, **1a** and **3**, react with a set of copper(I) arene complexes [(^{R}BDI^{Ar})Cu(η^2-toluene)$_n$] (**I–III**; **I**: R = CF_3, Ar = Mes, n = 0.5; **II**: R = Me, Ar = C_6F_6, n = 1; **III**: R = Me, Ar = 2,6-$Cl_2C_6H_3$, n = 0.5) bearing electron-deficient BDI ligands to form the corresponding σ-complexes (see Scheme 3).[38] All sets of copper complexes mentioned here bind reversibly to the monomeric three-coordinated zinc hydride complex [(^{Me}BDI^{Dipp})ZnH] (**3**).[38] Although the data support quick and reversible coordination in solution, it is possible to isolate crystalline forms of the resulting σ-complexes as [(^{R}BDI^{Ar})Cu(μ-H)Zn(^{Me}BDI^{Dipp})] (**5a–c**; **5a**: R = CF_3, Ar = Mes; **5b**: R = Me, Ar = C_6F_6; **5c**: R = Me, Ar = 2,6-$Cl_2C_6H_3$) from hydrocarbon solutions (Scheme 3).[38] These species were characterised by single-crystal X-ray diffraction studies, and the structure of **5c** showed a remarkably small Cu···Zn distance (2.4684(5) Å). The Cu···Zn distance follows the trend **5b** > **5a** > **5c** across the series. Interestingly, significant flexibility is observed in the coordination geometry at copper throughout the series. The data are indicative of a slight deviation from a distorted trigonal planar arrangement (in **5a** and **5b**) towards a T-shaped geometry (in **5c**, w.r.t. copper). In particular, the distortion towards a T-shaped geometry becomes more pronounced as the Cu···Zn separation decreases (**5b** > **5a** > **5c**). This is because the BDI ligands must undergo out-of-plane torsional rotation with each other to account for the approach of the two metals. Consequently, the geometry at copper bends from trigonal planar to a T-shaped geometry as the Zn–H ligand approaches copper, because the solid-state structures can withstand variations in the Cu···Zn distance of up to ±5% only. Upfield chemical shifts in low temperature ^{1}H NMR data support the presence of the σ-hydride in complexes **5a–c**.

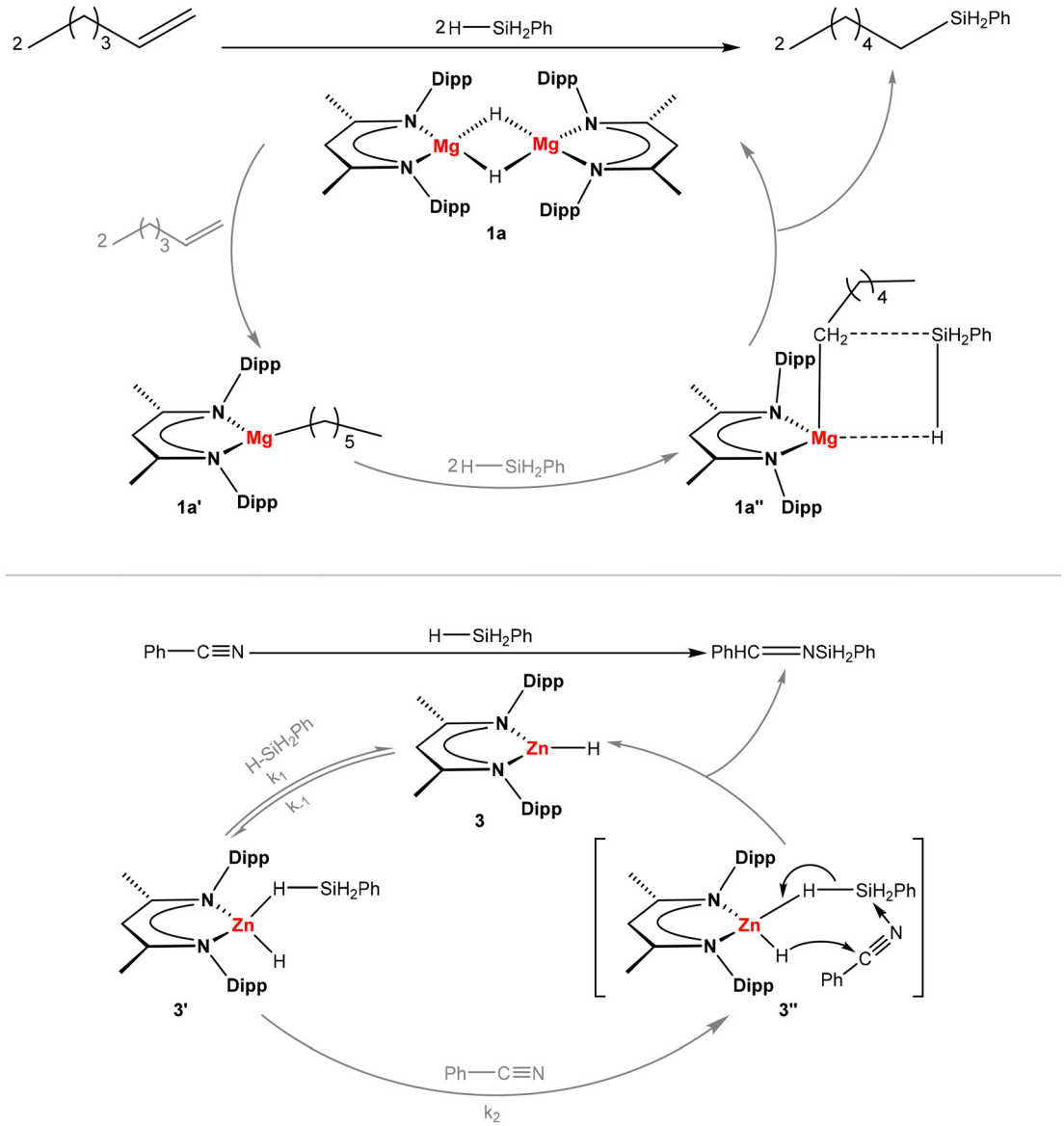

Scheme 2 Proposed cyclic mechanisms for catalytic hydrosilylation (with $PhSiH_3$) of (top) 1-hexene in the presence of **1a** and (bottom) benzonitrile in the presence of **3**.

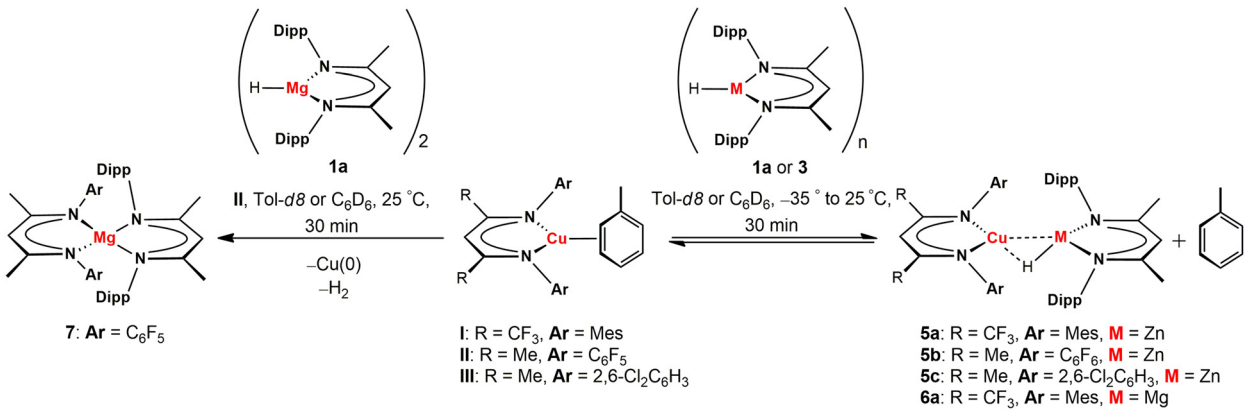

Scheme 3 Formation of σ-complexes **5a–c** and **6a** and the tetrahedral magnesium complex **7**; **1a**: M = Mg, *n* = 2; **3**: M = Zn, *n* = 1.

Unlike **5a–c**, the products of the reactions between dimeric molecular magnesium hydride [(^{Me}BDI^{Dipp})Mg(μ-H)$_2$] (**1a**) and copper(I) arene complexes (**I–III**) are unstable (Scheme 3).[38] In a hydrocarbon solution, they decompose readily within a few hours at ambient temperature. However, a σ-complex could be isolated and crystallographically characterized as [(^{R}BDI^{Ar})Cu(μ-H)Mg(^{Me}BDI^{Dipp})] (**6a**, R = CF_3, Ar = Mes) despite the frangible nature of the BDI ligand-supported Cu–H–Mg three-centre two-electron bonds (Scheme 3). The preparation and isolation of **6a** as a crystalline solid, isostructural with **5a**, was possible only when the reactions, followed by a work-up and direct crystallization, were carried out at significantly low temperatures of −35 °C. Multinuclear NMR spectroscopy was used to characterise the additional compounds that were generated *in situ* (Scheme 3). The reaction of **5b** with 0.5 equiv. of [(^{Me}BDI^{Dipp})Mg(μ-H)$_2$] (**1a**) enables the determination of at least one potential decomposition pathway. Although the formation of **6b** was not observed in this instance, the tetrahedral magnesium complex bearing two BDI ligands [(^{R}BDI^{Ar})Mg(^{Me}BDI^{Dipp})] (**7**; R = Me, Ar = C_6F_6) was generated cleanly (Scheme 3). An independent synthesis later reaffirmed the composition of complex **7**. It is most likely the result of an *in situ* ligand exchange reaction between magnesium and copper that produces "Cu–H" and [(^{R}BDI^{Ar})Mg(^{Me}BDI^{Dipp})]; the former easily breaks down into H_2 and copper(0).[38]

Alkene isomerisation: conversion of dienes to alkynes with a Zr/Zn heterobimetallic complex

Decades of research in the field of alkene isomerisation[39] have left the conversion of dienes into alkynes mostly obscure, with the dehydrogenation of alkenes to alkynes being the only known precedent.[40] Interestingly, the isomerization of cyclooctadiene to cyclooctyne is facilitated within the coordination sphere of an atypical Zr/Zn heterobimetallic complex [Cp_2ZrH(μ-H)$_2$Zn(^{Me}BDI^{Dipp})] (**8**) (Scheme 4).[41] For the sake of comparison, it should be mentioned that the isostructural Zr/Mg complex [Cp_2ZrH(μ-H)$_2$Mg(^{Me}BDI^{Dipp})] (**9**) or even Zr/Zr bimetallic complexes [Cp_2ZrH(μ-H)]$_2$ do not lead to trapping of the alkyne, but instead cause the expected isomerization of 1,5-cyclooctadiene (1,5-COD) to 1,3-cyclooctadiene (1,3-COD) (Scheme 4).[41]

The heterobimetallic M/Zr [M = Zn (**8**) or Mg(**9**)] complexes are the products of the simple addition reactions of the isostructural β-diketiminato hydrides [(^{Me}BDI^{Dipp})MH]$_n$ (**1a:** M = Mg, n = 2; **3:** M = Zn, n = 1) with [Cp_2ZrH_2]$_2$. Although complexes containing Zr–H–Mg groups have precedence although limited, those containing a Zr–H–Zn moiety were previously unknown. The reaction of the Zn/Zr complex (**8**) with 1,5-COD in C_6D_6 at 80 °C results in slow isomerisation of the hydrocarbon to 1,3-COD, along with the formation of a cyclooctyne-bound heterobimetallic complex **10** (Scheme 4) as a major product (85% yield). While the chemical shifts in the ^{1}H NMR spectrum account for the protons adjacent to the unsaturated C–C bond in **10**, ^{13}C NMR data provided downfield resonances typical of the alkynes. A single crystal X-ray diffraction experiment on **10** demonstrated the specific way in which cyclooctyne binds to the metal centres. This experiment may also provide insight into how the reactivity is dependent on the major group fragment. An alkyne ligand and a hydride bridge the two metal centres, zinc and zirconium. The Zr–C bond lengths agree with the alkyne bridge's predicted asymmetry. The length of the Zn–C bond (2.198(2) Å) is shorter than those reported for strongly *p*-coordinated alkene complexes of Zn^{II} (range: 2.2–2.3 Å), but it is slightly longer than the range found for terminal Zn–C σ-bonds (1.9–2.1 Å). The obtuse C–C–C bond angles (129.0(2) Å and 133.9(2) Å) and the short C–C bond length (1.308(3) Å) lend credence to the formulation as a coordinated cyclooctyne. In contrast, the related bimetallic complexes Zr/Mg (**9**) or [Cp_2Zr(μ-H)(H)]$_2$ give mixtures of 1,3-COD, cyclooctene, and cyclooctane from 1,5-COD. Therefore, the generation of a metal-bound cyclooctyne was observed only in the zinc analogue (**8**). This may be because the beneficial binding of cyclooctyne provides the thermodynamic driving force for the isomerisation. The role of stabilising interactions that permit cyclooctyne to bind to the heterobimetallic complex **8** is also emphasized by some control reactions.[41]

Hydrogen elimination from molecular zinc and magnesium hydride clusters: A comparison

The efficient hydrogen storage properties of early main-group metal hydrides have attracted significant interest.[42–45] Even though MgH_2 appears to be an ideal candidate for reversible hydrogen storage, its high thermodynamic stability presents a

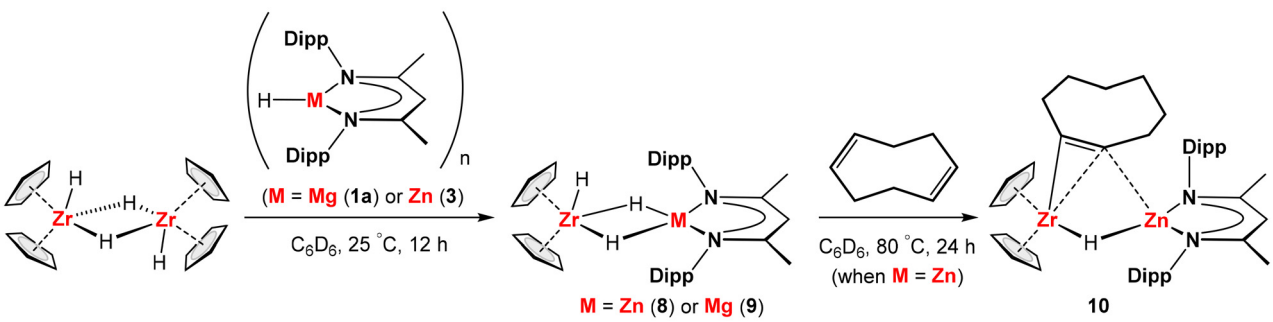

Scheme 4 Synthesis of heterobimetallic complexes **8** or **9** followed by formation of the cyclooctyne-bound heterobimetallic complex **10** with **8**.

challenge, which results in relatively high hydrogen desorption temperatures (300 °C) and sluggish hydrogen release and uptake kinetics.[44–46] It is interesting to note that some molecular clusters of magnesium and zinc have been shown to release hydrogen upon thermal decomposition at much lower temperatures.[47–49] For example, the dimeric magnesium and monomeric zinc hydrides $[(^{Me}BDI^{Dipp})MH]_n$ (**1a:** M = Mg, n = 2 and **3:** M = Zn, n = 1) show a record of thermal decomposition (or H_2 release) temperatures of 120 °C and 150 °C with the consecutive release of 1 and 0.5 equiv. of H_2, respectively (Scheme 5).[48,49] The higher stability of **3** due to its monomeric form accounts for its higher decomposition temperature than that of **1a**. The much larger magnesium hydride cluster [**NN**-$(MgH)_2]_2$ (**11**) (Scheme 5), supported by coupled BDI ligands, eliminates hydrogen at higher temperature (175 °C, Scheme 5) with a stoichiometric release of 2 equiv. of H_2.[48]

In stark contrast, the isostructural zinc cluster [**NN**-$(ZnH)_2]_2$ (**12**) demonstrated a significantly lower decomposition temperature (90 °C) with the release of 1.8 equiv. of H_2.[49] This is in accordance with the significantly higher decomposition temperature for MgH_2 (300 °C) *vs.* that for ZnH_2 (100 °C), which is likely attributable to the simpler reduction of Zn^{2+} with respect to Mg^{2+}.[49] According to calculations, the decomposition temperature of [**NN**-$(MgH)_2]_2$ (**11**) is much lower than that of bulk MgH_2 (175 *vs.* 300 °C).[48,49] However, this correlation between size and hydrogen-elimination temperatures is not immediately apparent in zinc hydride clusters. For instance, [**NN**-$(ZnH)_2]_2$ (**12**) and bulk ZnH_2 exhibit comparable stability with decomposition temperatures of 90 °C *vs.* 100 °C, respectively.[49] This could potentially be attributed to the more covalent nature of the Zn–H bond and/or the distinct solid-state structures of the bulk metal hydrides MgH_2 and ZnH_2 (the structure of ZnH_2 is unknown at present but is likely to be polymeric in nature).[49] The DFT calculations anticipate that the H_2 release from both clusters **11** and **12** propagates through the formation of low valent M(I) (M = Mn or Zn) clusters.[48,49] Although there are ongoing attempts for isolation and crystallization of the Mg^I species, attempts to isolate the corresponding Zn^I species have failed due to the decomposition to Zn^0.[48,49]

Comparison of magnesium and zinc in cationic π-arene and halobenzene complexes

The similarities and differences in magnesium and zinc chemistry were further established by the synthesis of Lewis base-free "naked" cationic magnesium and zinc complexes $[(^{tBu}BDI^{Dipp})M^+][B(C_6F_5)_4^-]$ [M = Mg (**13**) or Zn (**14**)] supported by the bulky $^{tBu}BDI^{Dipp}$ ligand and stabilized using the weakly coordinating anion $B(C_6F_5)_4^-$ and investigating their interactions with arenes or halobenzenes (Scheme 6).[50–52] Complexes **13** and **14** are synthesized by the reaction of the trityl tetrakis(pentafluoro phenyl)borate $[Ph_3C^+][B(C_6F_5)_4^-]$ with the metal alkyl complexes, *viz.*, $[(^{tBu}BDI^{Dipp})MR]$ (when M = Mg, R = *n*Bu; when M = Zn, R = Et) (Scheme 6).[50,51] The β-hydride abstraction leads to the formation of the cationic complex **13** or **14**; Ph_3CH and 1-butene or ethylene are by-products of the reaction.[50,51] In both cases, complex **13** or **14** could not be isolated as the ion pair $[(^{tBu}BDI^{Dipp})M^+][B(C_6F_5)_4^-]$ [M = Mg (**13**) or Zn (**14**)]. This may be due to the significant steric bulk of the $^{tBu}BDI^{Dipp}$ ligand, which intercepts an M···$(C_6F_5)_4B^-$ (M = Mg or Zn) interaction.[50–52] However, the solvent molecules are sufficiently small to interact with the Lewis acidic M^{2+} (M = Mg or Zn) centre(s) within the ligand's pocket.[50–52] Thus, a series of complexes with $(^{tBu}BDI^{Dipp})M^+$···arene cations (arene = benzene, toluene, xylene) or $(^{tBu}BDI^{Dipp})M^+$···XPh cations (X = F, Cl, Br, I) have been accessed.[51,52] All the crystal structures of the $(^{tBu}BDI^{Dipp})Mg^+$···arene complexes (arene = benzene, toluene, xylene; **15–17**) showcase η^2-coordination of the arene to the metal centre (Scheme 6).[51,52]

The $(^{tBu}BDI^{Dipp})Zn^+$···arene cations (arene = benzene (**18**), toluene (**19**)) bear strong resemblances to the structures of the analogous Mg cationic complexes **15–17**, whereas xylene in the $(^{tBu}BDI^{Dipp})Zn^+$···xylene cation (**20**) is bound to the metal in an

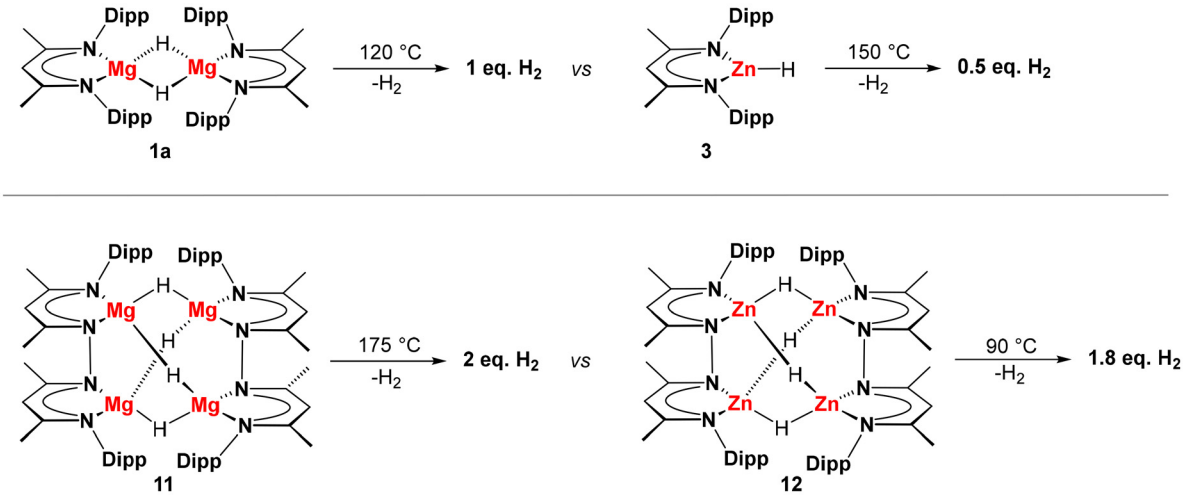

Scheme 5 Thermal decomposition of magnesium and zinc hydride clusters.

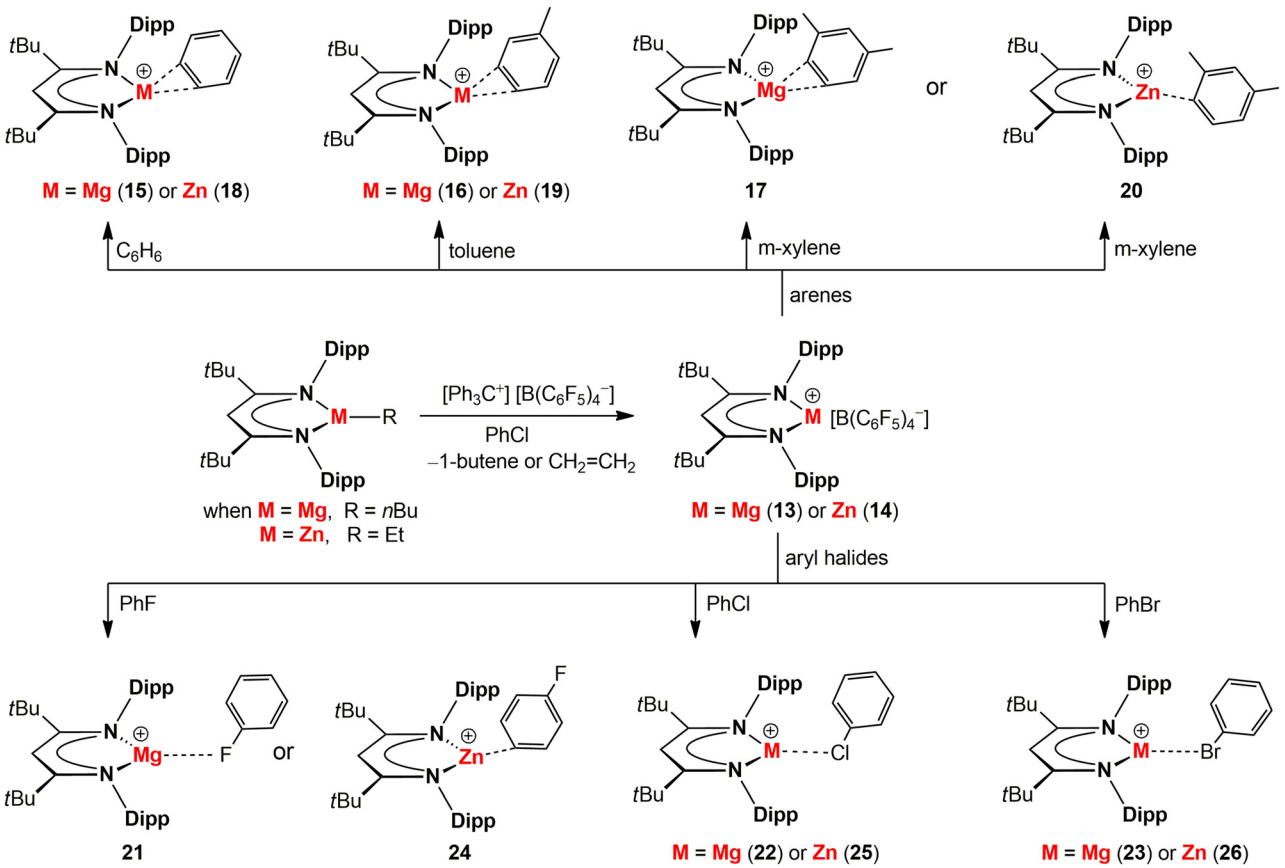

Scheme 6 Synthesis of the "naked" cationic magnesium and zinc complexes **13** and **14** and the [(^{tBu}BDI^{Dipp})M$^+$·(substrate)] [B(C$_6$F$_5$)$_4^-$] (M = Mg or Zn) complexes **15–26**.

η^1 fashion (Scheme 6).[51] This leads to the conclusion that regardless of the coordination numbers and ionic radii of Mg^{2+} and Zn^{2+} being similar, the structures of the cations of (^{tBu}BDI^{Dipp})Zn$^+$···arene and (^{tBu}BDI^{Dipp})Mg$^+$···arene are clearly different.[51] Compared to the equivalent Mg cations, the Zn cations exhibit metal···C(arene) bond lengths that are 0.1–0.2 Å shorter consistently.[51] This results from the increased electronegativity of zinc and its propensity to bind with ligands that significantly contribute covalently.[51] The longer Mg···arene interactions, on the other hand, have an electrostatic origin.[51,52]

A similar inference is reached when the Mg···XPh (X = F, Cl, Br; **21–23**) and Zn···XPh (X = F, Cl, Br; **24–26**) complexes are compared (Scheme 6).[51] For example, in comparison with the Mg···X distances, the Zn···X distances are consistently 0.1–0.2 Å shorter.[51] There is a noticeable distinction between Mg and Zn in terms of PhF complexation. Zn is reported to have a Zn···(π)PhF interaction, but Mg has a strong preference for Mg···FPh interactions (Scheme 6).[51] The HSAB theory explains that soft cations like Zn^{2+} are more likely to interact with soft Lewis bases like aromatic π-systems, while hard cations like Mg^{2+} prefer to interact with hard Lewis bases like fluorine.[51] According to DFT calculations, this trend is particularly noticeable for PhF but not as much for the heavier halobenzenes with softer halogen substituents such as chlorine or bromine.[51]

The hapticity of the arene ligands of compounds **15–20** and **24** can be compared based on the electron density on benzene rings and polarising ability of the metals in all the cases. A pattern emerges where arenes with higher electron density tend to coordinate to the metal in an η^1 fashion. This is observed, for example, when electron-donating groups such as fluorine, through resonance, or methyl groups, through inductive effects as seen in xylene, are present. On the other hand, arenes with lower electron density, such as benzene and toluene, are more likely to exhibit η^2 coordination in order to meet the electron demands of the metal centers. However, in compound **20**, zinc being more electronegative can polarize the π-electron cloud more in order to satisfy its electron density, which is presumably the reason for xylene to show the η^1 donation mode.

Synthesis of a magnesium–amidoborane complex and its role in catalytic formation of a new bis(aminoborane) ligand

Early main group metal amidoborane compounds, *viz.*, $LiNH_2BH_3$, $NaNH_2BH_3$, and $Ca(NH_2BH_3)_2$, were considered potential hydrogen storage materials a decade ago.[53,54] Compared to the standard ammonia-borane NH_3BH_3, the

removal of molecular hydrogen in these compounds offers several benefits. These include near-thermoneutrality and a much lower hydrogen release temperature. However, both metal amidoborane and ammonia borane face challenges in the development of a reversible hydrogen uptake process.[55]

The studies on the mechanism of hydrogen release in alkaline-earth metal amidoborane complexes directed interest in studying plausibly related zinc amidoborane complexes. Instead of the anticipated zinc amidoborane complex, the straightforward salt metathesis reaction between potassium amidoborane, $KNH(iPr)BH_3$ and the BDI supported zinc chloride [(^{Me}BDI^{Dipp})ZnCl] produced the zinc hydride [(^{Me}BDI^{Dipp})ZnH] (**3**) in a good yield (71%, Scheme 7).[56] It is, however, speculated that the desired zinc amidoborane complex [(^{Me}BDI^{Dipp})Zn{NH_2(iPr)BH_3}] (**27**) is probably the intermediate, which upon β-hydride elimination followed by the production of several derivatives of ammonia borane as oligomeric species (many signals were detected in the NMR spectra) leads to the clean formation of the zinc hydride complex **3** (Scheme 7).[56]

Succeeding this, the synthesis of a magnesium amidoborane complex [(^{Me}BDI^{Dipp})Mg{NH(Dipp)BH_3}] (**28**) with a large substituent on nitrogen was studied to gain insight into the impact of the metal on the stability and breakdown of metal amidoborane complexes in general.[55] The reaction of the heteroleptic magnesium complex [(^{Me}BDI^{Dipp})Mg{N($SiMe_3$)$_2$}] with the ammonia borane derivative $NH_2(Dipp)BH_3$ resulted in a catalytic decomposition of the latter to a new bis(amino) borane compound $HB[NH(Dipp)]_2$, probably following the route shown in Scheme 7.[55] As this bis(amino)borane compound can be doubly deprotonated to a potentially useful dianionic boraaminate (bam) ligand, $HB[N(Dipp)]_2^{2-}$, a convenient and atom-efficient route was developed.[55] Therefore, the synthesis of the magnesium–amidoborane complex (**28**) and its possible role in the formation of the new bis(amino) borane compound probably take place through the formation of complexes **28′**, **28″** or the highly reactive magnesium hydride reagent [(^{Me}BDI^{Dipp})MgH] (**28‴**), as illustrated in Scheme 7.[55]

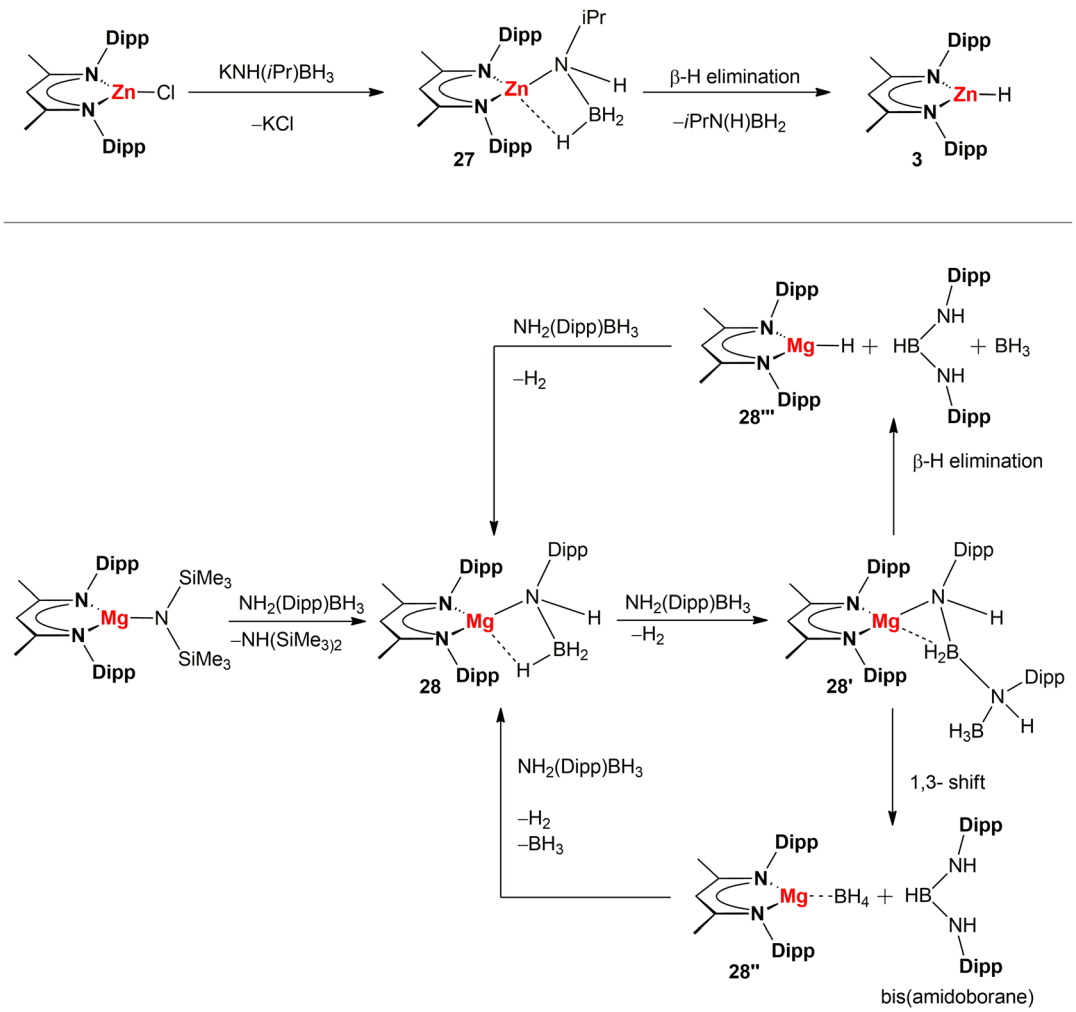

Scheme 7 Top: Possible route for the synthesis of the monomeric zinc hydride complex **3** *via* β-hydride elimination of the zinc amidoborane complex **27**. Bottom: Synthesis of the magnesium amidoborane complex **28** and the possible cyclic routes for the formation of the new bis(aminoborane) ligand in the presence of **28**.

3. N-heterocyclic carbenes as ligands

Bulky anionic ligands such as the BDI ligand and its derivatives (*vide supra*) or ligands based on neutral N-heterocyclic carbenes (NHC) largely aid the steric protection of the metal–hydrogen bonds in magnesium and zinc hydrides.[57,58] These anionic or neutral co-ligands lower the aggregation and greatly enhance the solubility, thus improving reactivity. NHCs can also stabilize relatively large mixed magnesium/zinc hydride clusters. These clusters are generated by treating the respective metal precursors with hydride sources like dimethylamine borane (DMAB) and phenylsilane ($PhSiH_3$) in the presence of NHCs such as IPr (IPr = 1,3-bis(2,6-di-isopropylphenyl)imidazol-2-ylidene).[59] For example, by reacting the zinc bis(amide) $Zn(HMDS)_2$ (HMDS = hexamethylsilazide) with an equal stoichiometry of DMAB in the presence of IPr, an NHC-stabilised mixed amido-hydride zinc cluster $Zn_4(HMDS)_2H_6$·IPr (**29**) could be accessed (Scheme 8). A tetranuclear adamantyl-like $\{Zn_4H_6\}^{2+}$ core was identified through synchrotron single-crystal X-ray diffraction.[59] The core is a tetrahedral Zn_4 cluster, with the six hydride ligands slightly displaced from the six boundaries of the tetrahedron.[59] Each hydride acts as a bridge between two zinc centres. The isostructural magnesium analogue of cluster **29**, $Mg_4(HMDS)_2H_6$·IPr (**30**), was synthesized by the reaction of $Mg(HMDS)_2$·IPr with $PhSiH_3$ (Scheme 8).[60] The shorter metal–hydride, metal–amide, and metal–carbene bond lengths in the zinc cluster **29** than those in its magnesium analogue **30** can be rationalised as owing to the reduced size of zinc (covalent radius of 1.22 Å for Zn *vs.* 1.41 Å for Mg).[59,60] This is most apparent in the Zn–carbene bonds, which have an ~8% shorter mean value of 2.038 Å *vs.* 2.2063 (19) Å in the magnesium cluster (**30**).[59] It should be noted that attempts to synthesize **29** using a similar approach to that of **30** led to the formation of a mononuclear mixed hydridoamido zinc complex Zn(HMDS)H·IPr (**31**) (Scheme 8).[59]

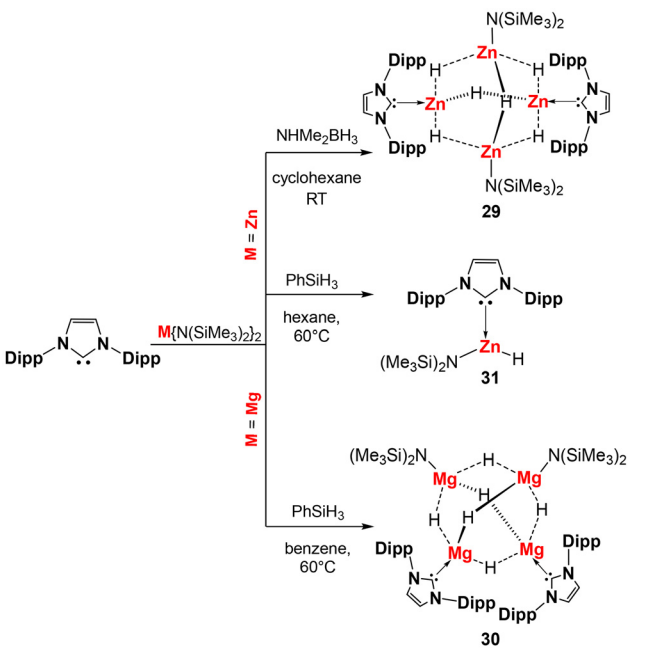

Scheme 8 Synthesis of NHC-coordinated zinc and magnesium hydride clusters, **29** and **30**, along with a mononuclear mixed hydridoamido zinc complex, **31**.

4. NNNN-type-macrocyclic ligands

The tripodal macrocyclic ligands of the NNNN-type such as tris{2-(dimethylamino)ethyl}amine (Me_6TREN) can stabilise precarious systems such as s-block metal complexes.[61,62] Isolation of unique cationic complexes of magnesium and zinc [LMR][A] (**32–35**; **32**: M = Mg, L = Me_6TREN, R = *n*-Bu, A = $[B(C_6F_5)_4^-]$; **33**: M = Zn, L = Me_6TREN, R = Et, A = $[B\{C_6H_3(CF_3)_2\}_4^-]$; **34**: M = Mg, L = *N*,*N*′,*N*″,*N*‴-pentamethyldiethylenetriamine (PMDTA), R = *n*-Bu, A = $[B\{C_6H_3(CF_3)_2\}_4^-]$; **35**: M = Zn, L = PMDTA, R = Et, A = $[B(C_6F_5)_4^-]$) is also achieved by the reactions of the respective metal alkyls with the ligand Me_6TREN or PMDTA in the presence of the Brønsted acid $[PhNMe_2H][B(C_6F_5)_4]$ or $[Ph_2NMeH]$ $[B\{C_6H_3(CF_3)_2\}_4]$ (Scheme 9).[63–66] While the molecular structures of **32** and **33** revealed κ^4 coordination of Me_6TREN to the metal centres resulting in a distorted trigonal pyramidal arrangement of the donor atoms around them, complexes **34** and **35** were revealed to have a κ^3 coordination of PMDTA and a consequent tetrahedral geometry at zinc. The structural identities of all the complexes were corroborated by NMR spectroscopy.[63,64,66]

The ethylzinc cationic complexes **33** and **35** further led to the formation of respective hydridozinc cationic species [LZnH][A] (**36** and **37**; **36**: L = Me_6TREN, A = $[B\{C_6H_3(CF_3)_2\}_4]$; **37**: L = PMDTA and A = $[B(C_6F_5)_4]$), respectively, on treatment with triphenylsilanol (Ph_3SiOH) followed by reacting the generated zinc siloxide species with phenylsilane ($PhSiH_3$) (Scheme 9).[64,66] The corresponding hydridomagnesium cation $[(PMDTA)MgH]_2$ $2[B\{C_6H_3(CF_3)_2\}_4]$ (**38**) could be accessed by the reaction between a diethyl ether solution of **34** and hydride sources such as HBpin or excess $PhSiH_3$ (Scheme 9).[65] SC-XRD studies confirmed the structural analogies of the cationic hydridozinc complexes **36** and **37** with their respective precursors **33** and **35**.[64,66] ^{1}H NMR studies revealed shielded hydride and κ^4 and κ^3 coordination of Me_6TREN and PMDTA to the zinc centres in **36** and **37**, respectively. In contrast, the magnesium complex **38** was found to have a dimeric structure with two hydrides bridged between two trigonal bipyramidal magnesium centres.[64–66]

The reactivity of the alkyl-magnesium and zinc cations, **32** and **33**, towards electrophiles is distinct from one another. For example, the butylmagnesium cation **32** effectively alkylates CO_2 akin to typical Grignard reagents, leading to the formation of a cationic magnesium carboxylate $[Me_6TREN\text{-}Mg\text{–}O\text{–}C(n\text{-}Bu)O]_2\cdot 2[B(C_6F_5)_4^-]$ (**39**) (Scheme 10; top).[63] However, it quantitatively reduces Ph_2CO, revealing the hydridic nature of the β-CH functionality in **32** (Scheme 10; bottom).[63] This leads to the conclusion that the abstraction of the β-CH of [Me_6TREN-Mg-

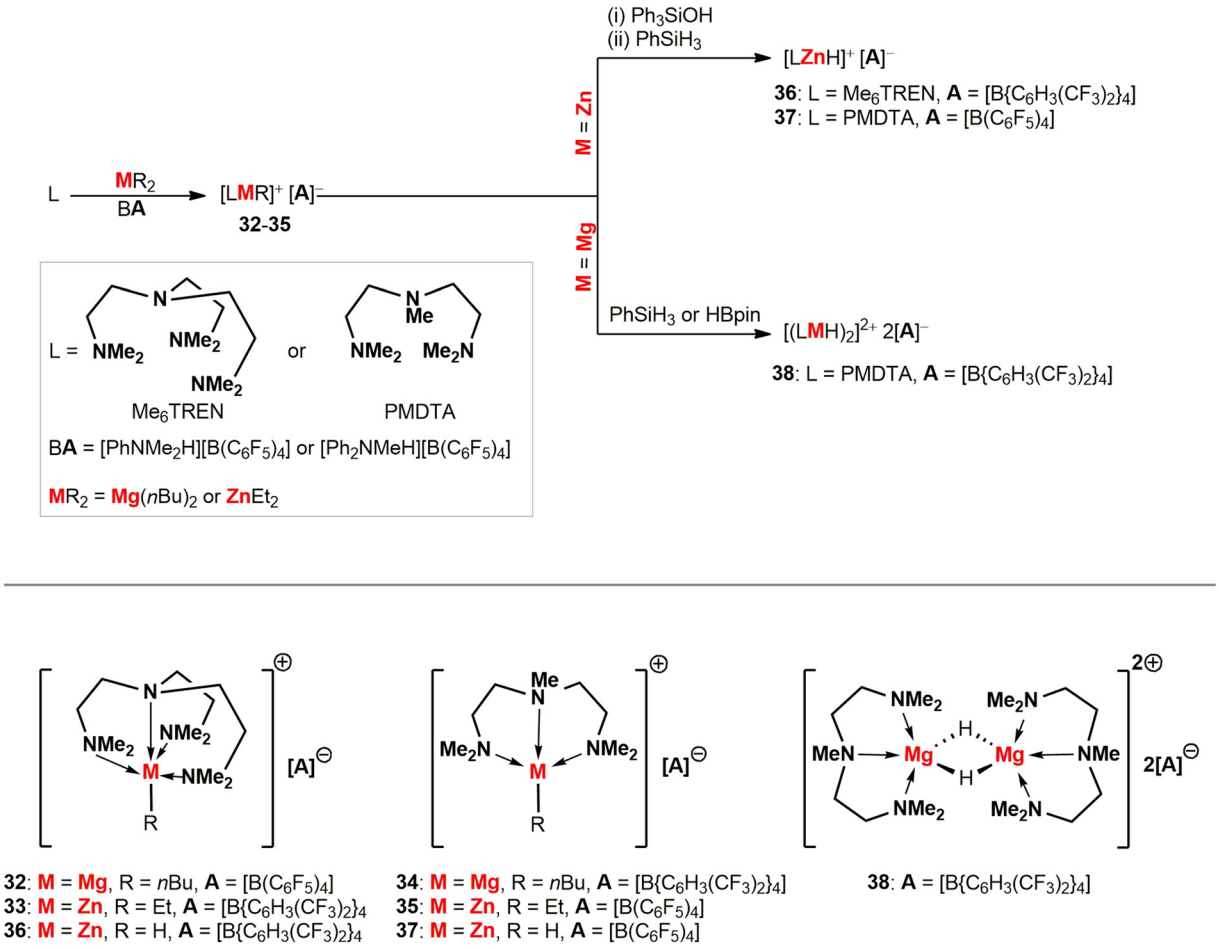

Scheme 9 Synthesis of cationic complexes of magnesium and zinc, **32–38**.

n-Bu]$^+$ is preferred over alkylation depending on the nature of the incoming electrophile and solvent polarity.[63] To illustrate, Ph_2CO gets partially reduced in THF, affording both the alkylated product **40** and the reduced product **41** (Scheme 10, bottom), whereas it yields **41** as a single product in toluene. This is due to the stabilisation of the cyclic six-membered transition state in the reduction pathway by a non-polar solvent.[63] Unlike **32**, the ethylzinc cation **33** does not react with Ph_2CO, thus proving that the β-CH in **33** is inactive because the Mg–C in **32** is more polar than the Zn–C in **33**.[64]

In contrast to the reactivity of the disguised hydride in the butylmagnesium cation **32**, the thermally stable hydridozinc cation **36** instantaneously reduces CO_2 and Ph_2CO, resulting in the formate complex (**42**) and the alkoxyzinc complex (**43**), respectively (Scheme 10).[64] In addition, as illustrated in Scheme 11, **36** was found to act as a catalyst in the presence of the mild Lewis acid triphenylborane (BPh_3) for the rare selective hydrosilylation of CO_2 using $PhSiH_3$.[64] It should be mentioned that **36** also shows moderate reactivity towards CO_2 hydrosilylation independently.[64] However, despite reduced ligand denticity, the four coordinate [(PMDTA)ZnH]$^+$ (**37**) does not do so since it forms a stable dimeric zinc formate (**44**) upon reaction with CO_2, and hence, the presence of mild Lewis acids like BPh_3 is essential to generate the monomeric zinc formate, thereby facilitating hydrosilylation.[66] Interestingly, the instantaneous reduction of Ph_2CO in C_6D_6 revealed the hydridic nature of the dimeric magnesium congener of **37**, $[(PMDTA)MgH]_2^+$ (**38**). However, further reactivities continue to be challenging due to the unstable nature of the complex.[65]

5. Anionic nitrogen donor-type ligands

Ligands with anionic nitrogen as donor atoms have a precedence as co-ligands for stabilising CO_2 hydrosilylation catalysts based on Earth abundant non-precious metals. For example, a tris(2-pyridylthio)methyl zinc hydride complex, [κ^3-Tptm]ZnH, was found to be an effective catalyst for the hydrosilylation of CO_2 to the silyl formate, $HCO_2Si(OEt)_3$.[67–69] Similarly, the structurally related tris[(1-isopropylbenzimidazol-2-yl)dimethylsilyl]methyl ligand [Tism$^{(iPr)Benz}$] was utilized to support the terminal zinc and magnesium

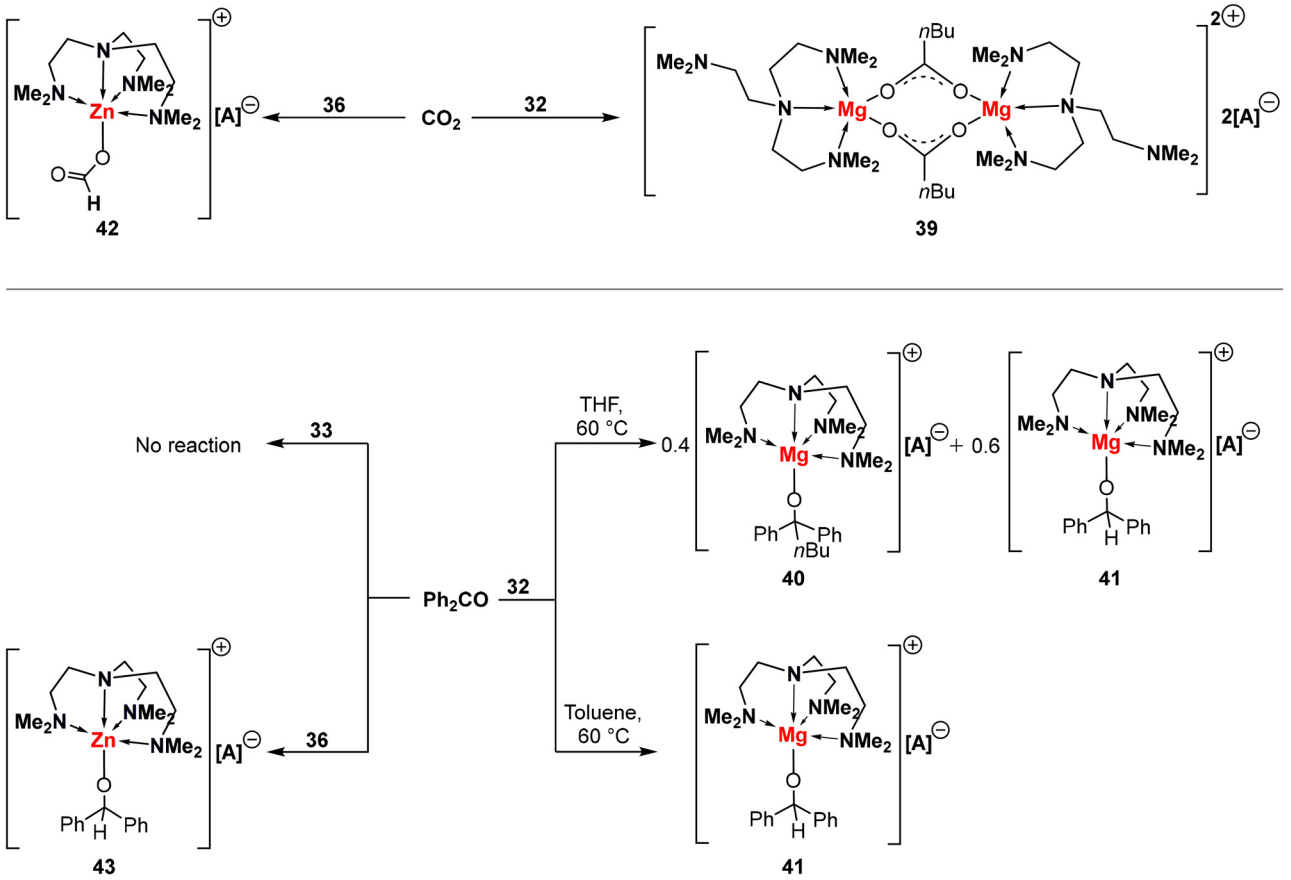

Scheme 10 Reactivity of the *n*-butylmagnesium cation **32** and the hydridozinc cation **36** towards electrophiles like CO_2 (top) and Ph_2CO (bottom).

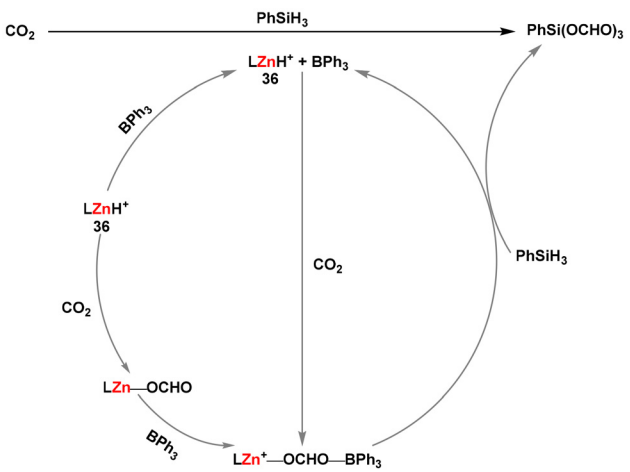

Scheme 11 Proposed catalytic cycle for the selective hydrosilylation of CO_2 using $PhSiH_3$ in the presence of the hydridozinc cation **36** and triphenylborane.

hydride complexes [κ^3-Tism $^{(iPr)Benz}$]MH [M = Zn (**45**) and M = Mg (**46**)].[70] Both **45** and **46** reacted with tris(pentafluorophenyl)borane [$B(C_6F_5)_3$] generating the ion pairs {[Tism$^{(iPr)Benz}$]M}[$HB(C_6F_5)_3$] (**47**: M = Zn, **48**: M = Mg) as rare examples of these metals in trigonal pyramidal coordination environments. It is important to note that (i) zinc and magnesium hydrides **45** and **46** do not independently catalyse the hydrosilylation of CO_2 by $PhSiH_3$, rather a catalytic system is achieved in the presence of $B(C_6F_5)_3$; (ii) the magnesium hydride complex **46** provides a more efficient catalytic system in the presence of $B(C_6F_5)_3$ and represents the first example of catalytic hydrosilylation of CO_2 by a magnesium complex.[70] Specifically, the zinc and magnesium ion pairs [{Tism$^{(iPr)Benz}$}M][$BH(C_6F_5)_3$], **47** and **48**, are differ in their reactivity towards CO_2 despite their analogous identities. As illustrated in Scheme 12, the magnesium complex **48** reacts promptly with CO_2, yielding the formatoborate derivative [Tism$^{(iPr)Benz}$]$MgOC(H)OB(C_6F_5)_3$ (**49**).[70] However, the zinc compound **47** does not form a detectable product under identical conditions. However, the formato bis(borate) species {[Tism$^{(iPr)Benz}$]M}[$HC\{OB(C_6F_5)_3\}_2$] [M = Zn (**50**) or Mg (**51**)] were detected for both metals upon further reaction of the formatoborate derivative(s) with another molecule of $B(C_6F_5)_3$. The release of the silylformate R_3SiCO_2H and regeneration of the ion pairs **47** or **48** is the final sequence of the catalytic cycle, followed by the reduction of R_3SiCO_2H to CH_4 (Scheme 12). It is worth mentioning that although other metal complexes are reported to serve as catalysts for CO_2 hydrosilylation in combination with $B(C_6F_5)_3$, the zinc and

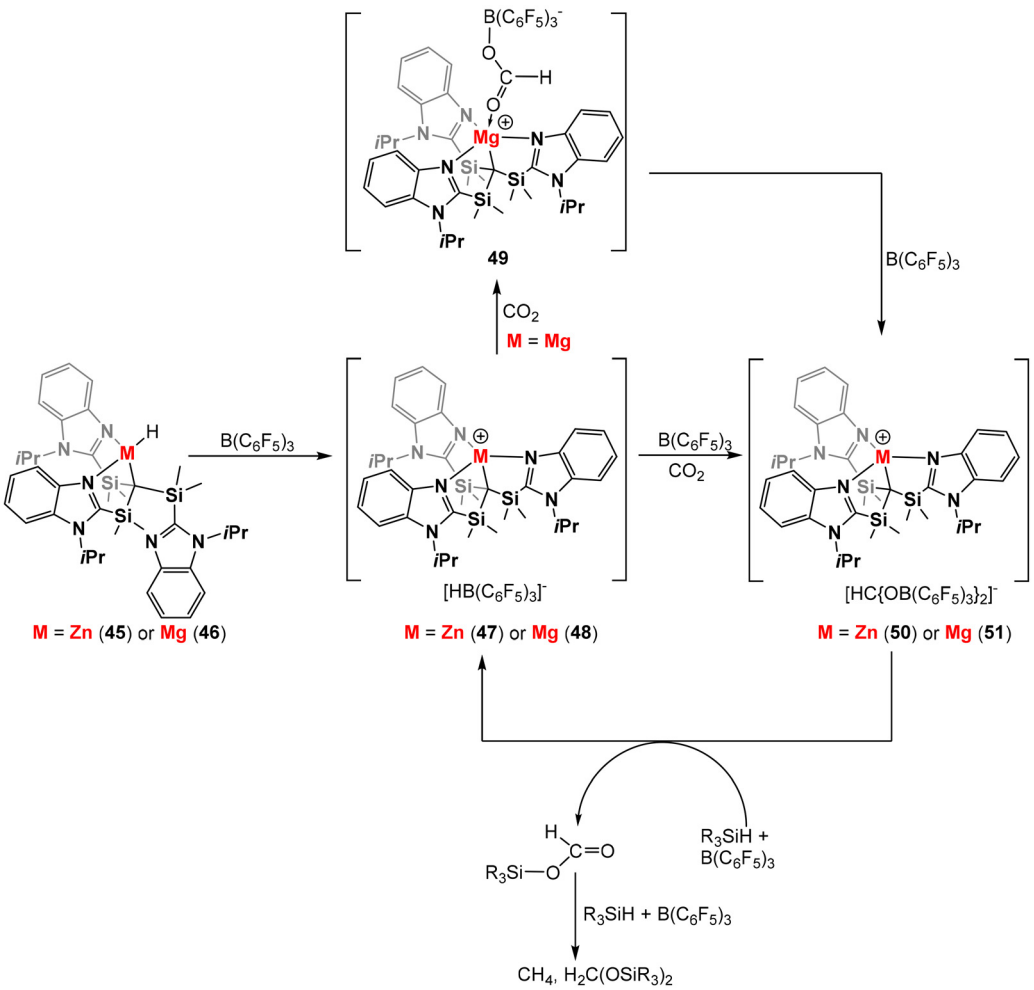

Scheme 12 Possible catalytic cycle for the hydrosilylation of CO_2 in the presence of **45** or **46** together with tris(pentafluorophenyl)borane.

magnesium systems **47** and **48** supported by anionic nitrogen donor-type ligands utilize Earth-abundant and non-toxic main group metals and most importantly are active at ambient temperatures. In particular, the magnesium system **48** is highly resilient and can be recycled multiple times without an appreciable decrease in activity.[70]

6. Allyl anions as ligands

It is essential in organometallic chemistry to explore the entire spectrum of interactions of delocalised π-electron systems with metal centres, *viz.* from ionic to covalent bonds.[36,71] The allyl group serves as the simplest example of a delocalised π-electron system and is, therefore, a model ligand for such studies.[72] It is mostly distinguished by its versatile reactivity and coordination modes in metal complexes (**A–F**; Scheme 13, top).[73,74] Magnesium complexes exhibit a broad range of structural variations of allyl-supported metal complexes.[75] This is most likely due to the fine balance between covalent and ionic bonding and the accessibility of complexes ranging from cat-

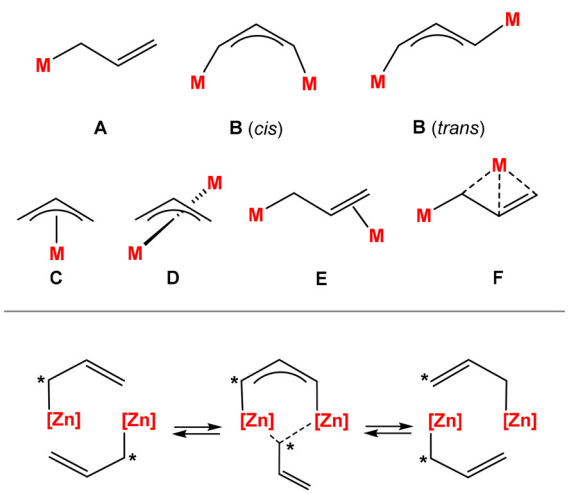

Scheme 13 Top: some of the identified coordination modes of the allyl ligand concerning metal–carbon interactions of σ-type (**A**: η^1, **B**: μ_2-η^1:η^1 (*cis* or *trans*)), π-type (**C**: η^3, **D**: μ_2-η^3:η^3) or σ-type and probably π-type (**E**: μ_2-η^1:η^2, **F**: μ_2-η^1:η^3). Bottom: intermolecular mechanism for allyl exchange in zinc–allyl complexes.

ionic, neutral, anionic or dianionic to cluster frameworks.[75,76] For instance, among the six structurally validated coordination modes of the allyl ligand concerning metal–carbon interactions (Scheme 13, top) of σ-type (**A**: η^1, **B**: μ_2-η^1:η^1 (*cis* or *trans*)), π-type (**C**: η^3, **D**: μ_2-η^3:η^3) or σ-type and probably π-type (**E**: μ_2-η^1:η^2, **F**: μ_2-η^1:η^3), magnesium–allyl complexes like the parent compound bis(allyl)magnesium [$Mg(C_3H_5)_2$] (**52**) generally favour σ-type interactions (**A** or **B**; Scheme 13, top).[72,75,76] These interactions can be noted as the η^1 coordination mode of the allyl ligand, both in solution and solid states.[72] However, as per DFT calculations for **52**, π-type interactions (**C** or **D**; Scheme 13, top) are also probable in the absence of a donor solvent.[75,76] Recent advances also highlight the formally charged magnesium–allyl compounds with charges ranging from +1 to −2 at the magnesium centre, showcasing a novel coordination mode of the allyl ligand in the solid state, *viz.*, the μ_3-η^1:η^3:η^3 bond in addition to interesting reactivities.[75,76]

Zinc–allyl complexes, on the other hand, exhibit an even broader scope of coordination modes, *viz.*, σ-type (**A**), π-type (**C**), along with both σ-type and/or π-type (**D**).[72,75] While it was perceived that the allyl ligands of the parent bis(allyl)zinc [$Zn(C_3H_5)_2$] (**53**) complex are in the η^3 bonding situation in the solid state, SCXRD data for the complex reveal a μ_2-η^1:η^1 coordination mode.[72,75] This demonstrated that exclusively π-type interactions are not favoured in zinc–allyl complexes.[72] Rather, the Lewis acidic divalent zinc centres in these complexes exhibit two σ-type bonding modes of allyl ligands, *cis*- and *trans*-**B** (Scheme 13, top).[72,75] Additionally, *ab initio* calculations have suggested σ-type coordination modes in **53** in the gas phase.[72] At room temperature, the allyl ligand exhibits fluxional behaviour in solution, but an η^1 coordination state can be preserved at low temperatures.[77] Monocationic and monoanionic allylzinc complexes also exhibit σ-type zinc–allyl interactions in the solid state.[77–79] The dynamic behaviour of zinc–allyl complexes in solution can be understood by looking at various coordination modes.[72] For instance, bis(allyl)zinc (**53**) as well as its cationic or anionic counterparts undergo rapid allyl exchange.[80] The mechanism of allyl exchange for **53** has been studied in THF. It follows second-order kinetics associated with an intermolecular allyl-exchange mechanism involving a transition state with a μ_2-η^1:η^1 coordination mode like the solid-state structure of **53** (Scheme 13, bottom).[80] This interpretation is supported by the aversion of allyl zinc compounds to π-type metal–allyl interactions.[72] The order of the allyl-exchange rate in solution is cationic < neutral < anionic.[75]

One of the most distinctive and well-known characteristics of metal–allyl complexes is their ability to interact with electrophiles at both C termini.[75] Among the allyl-specific reactivities, the dearomatisation of pyridines to access pharmacologically active N-metalated dihydropyridines (DHPs) have been reported for both zinc– and magnesium–allyl complexes.[77,81] Reactions between metal–allyl complexes and pyridine in general involve an initial adduct formation by the coordination of pyridine (**Py**) at the metal centre followed by subsequent 1,2- or 1,4-carbometalation of pyridine leading to the desired N-metalated DHP.[75] The latter step being metal-dependent and specific. While the parent neutral bis(allyl)zinc [$Zn(C_3H_5)_2$] (**53**) complex reportedly reacts with pyridine leading to formation of the adduct [$Zn(C_3H_5)_2$]·(**Py**)$_2$ (**54**) but without subsequent carbometallation, the cationic magnesium–allyl complex [$Mg(C_3H_5)(THF)_5$][$B(C_6F_5)_4$] (**55**) leads to the 1,2-carbometalation of pyridine (Scheme 14).[77,81] However, product isolation was unsuccessful due to rapid decomposition.[81]

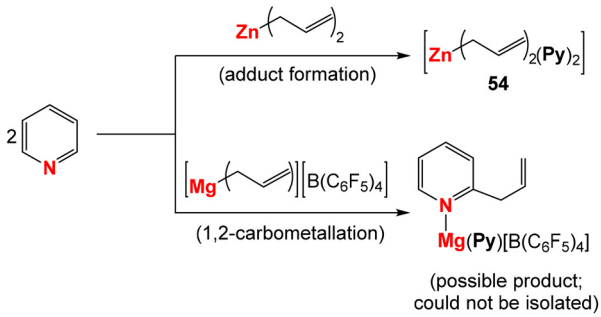

Scheme 14 De-aromatisation of pyridine in presence of the bis(allyl) zinc [$Zn(C_3H_5)_2$] (**53**) *vs.* cationic magnesium–allyl complex [$Mg(C_3H_5)(THF)_5$][$B(C_6F_5)_4$] (**55**).

Furthermore, the cationic zinc–allyl complex [$Zn(C_3H_5)(THF)_3$][$B(C_6F_5)_4$] (**56**) by virtue of a more Lewis acidic zinc centre participates in oxidatively induced allyl coupling.[78] Complex **56** undergoes reversible, solvent-dependent dimerization processes. Nearly quantitative yields of the dimetalated dimerization products were obtained. This reaction serves as a model for the dimerization of propene to an industrially significant (co)monomer 4-methylpent-1-ene, which is catalysed by alkali metals.[78] On the other hand, butadiene (BD) polymerisation was studied in the presence of magnesium-allyl initiators to determine how the charge at the metal centre affected the polymerisation.[81] Although anionic and dianionic magnesium–allyl complexes produce polybutadiene (PDB) with low polydispersity indices (PDIs) of 1.04–1.10 and high 1,2-PDB contents of 69–77%, neutral and cationic magnesium–allyl complexes like **52** and **55**, on the other hand, do not initiate polymerisation of BD. These reaction rates have a strong counterion effect (Ca ≪ K) and follow the order monoanionic < dianionic.[81]

7. Conclusions

The (near)isostructural magnesium and zinc complexes provide a means to compare several of these complementary and/or contrasting chemical behaviours through their structural aspects and/or chemical reactivities. The hard and soft nature of magnesium and zinc, respectively, leading to differences in Lewis acidity, is at the root of contrasting reactivity patterns of these complexes in alkene isomerisation, hydrosilylation of alkenes, nitriles or in their reactivities towards electrophiles like CO_2 and Ph_2CO, as well as interaction with solvents like xylene and fluorobenzene. The steric and electronic features of the ligands play an important role in generat-

ing and stabilizing these complexes. In this review, we have attempted to look at the interesting and rich chemistry of these complexes, which, in addition to their unique reactivities, have the potential to form diverse structural networks and play a larger role in environmentally valuable catalytic transformations, and thereby represent a fructuous area of study for chemists.

Author contributions

The manuscript was written with contributions from all authors. All authors have approved the final version of the manuscript.

Conflicts of interest

There are no conflicts to declare.

Data availability

Not applicable.

Acknowledgements

We thank IISER Thiruvananthapuram for the infrastructural facilities. A. V. thanks the Science and Engineering Research Board, Government of India (CRG/2023/004024), for generous funding.

References

1 R. D. Shannon, *Acta Crystallogr., Sect. A*, 1976, **32**, 751–767.
2 *Encyclopedia of Inorganic Chemistry*, ed. R. B. King, Wiley-VCH, 2nd edn, 2006.
3 A. F. Hollemann and N. Wiberg, *Lehrbuch Der Anorganischen Chemie*, De Gruyter, 102nd edn, 2007.
4 G. Srinet, R. Kumar and V. Sajal, *AIP Conf. Proc.*, 2013, **1536**, 247–248.
5 J. Intemann, *Magnesium and Zinc Hydride Complexes: From Fundamental Investigations to Potential Applications in Hydrogen Storage and Catalysis*, Rijksuniversiteit Groningen, 2014.
6 J. A. Garden, P. K. Saini and C. K. Williams, *J. Am. Chem. Soc.*, 2015, **137**, 15078–15081.
7 M. Chisholm, N. W. Eilerts, J. C. Huffman, S. S. Iyer, M. Pacold and K. Phomphrai, *J. Am. Chem. Soc.*, 2000, **122**, 11845–11854.
8 M. R. Hill, P. Jensen, J. J. Russell and R. N. Lamb, *J. Chem. Soc., Dalton Trans.*, 2008, **20**, 2751–2758.
9 A. B. Goel, S. Goel and E. C. Ashby, *Inorg. Chem.*, 1979, **18**, 1433–1436.
10 J. Intemann, P. Sirsch and S. Harder, *Chem. – Eur. J.*, 2014, **20**, 11204–11213.
11 R. M. Fabicon, A. D. Pajerski and H. G. Richey Jr., *J. Am. Chem. Soc.*, 1991, **113**, 6680–6681.
12 H. Tang, M. Parvez and H. G. Richey Jr, *Organometallics*, 2000, **19**, 4810–4819.
13 J. M. Grevy, Zinc: Organometallic Chemistry, in *Encyclopedia of Inorganic Chemistry*, ed. R. B. King, Wiley-VCH, 2nd edn, 2006.
14 E. von Frankland, *Ann. Chem. Pharm.*, 1849, **71**, 171–213.
15 E. Frankland, *J. Chem. Soc.*, 1850, **2**, 263–296.
16 V. Grignard, *Sci. Med.*, 1901, **6**, 1–118.
17 W. A. Nugent, *Chem. Commun.*, 1999, 1369–1370.
18 T. Rasmussen and P.-O. Norrby, *J. Am. Chem. Soc.*, 2001, **123**, 2464–2465.
19 A. B. Charette, A. Gagnon and J.-F. Fournier, *J. Am. Chem. Soc.*, 2002, **124**, 386–387.
20 *Zinc Catalysis*, ed. S. Enthaler and X.-F. Wu, Wiley-VCH, 2015.
21 D. Mukherjee and J. Okuda, *Angew. Chem., Int. Ed.*, 2018, **57**, 1458–1473 and references therein.
22 A. K. Wiegand, A. Rit and J. Okuda, *Coord. Chem. Rev.*, 2016, **314**, 71–82 and references therein.
23 Ankur, S. Kundu, S. Banerjee and A. Venugopal, Magnesium Complexes in Organic Synthesis, in *Comprehensive Organometallic Chemistry IV*, ed. G. Parkin, K. Meyer and D. O'hare, Elsevier, 2022, pp. 78–103.
24 L. Bourget-Merle, M. F. Lappert and J. R. Severn, *Chem. Rev.*, 2002, **102**, 3031–3066.
25 R. L. Webster, *Dalton Trans.*, 2017, **46**, 4483–4498.
26 C. Camp and J. Arnold, *Dalton Trans.*, 2016, **45**, 14462–14498.
27 C. Chen, S. M. Bellows and P. L. Holland, *Dalton Trans.*, 2015, **44**, 16654–16670.
28 D. C. H. Do, A. Keyser, A. V. Protchenko, B. Maitland, I. Pernik, H. Niu, E. L. Kolychev, A. Rit, D. Vidovic, A. Stasch, C. Jones and S. Aldridge, *Chem. – Eur. J.*, 2017, **23**, 5830–5841.
29 D. Leitner, B. Wittwer, F. R. Neururer, M. Seidl, K. Wurst, F. Tambornino and S. Hohloch, *Organometallics*, 2023, **42**, 1411–1424.
30 S. P. Green, C. Jones and A. Stasch, *Angew. Chem., Int. Ed.*, 2008, **47**, 9079–9083.
31 J. Spielmann, D. F. J. Piesik and S. Harder, *Chem. – Eur. J.*, 2010, **16**, 8307–8318.
32 S. Schulz, D. Schuchmann, M. Bolte, M. Kirchner, R. Boese, J. Spielmann and S. Harder, *Z. Naturforsch., B:J. Chem. Sci.*, 2009, **11–12**, 1397–1400.
33 J. Spielmann, D. Piesik, B. Wittkamp, G. Jansen and S. Harder, *Chem. Commun.*, 2009, **23**, 3455–3456.
34 S. J. Bonyhady, C. Jones, S. Nembenna, A. Stasch, A. J. Edwards and G. J. McIntyre, *Chem. – Eur. J.*, 2010, **16**, 938–955.
35 L. Garcia, C. Dinoi, M. F. Mahon, L. Maron and M. S. Hill, *Chem. Sci.*, 2019, **10**, 8108–8118.
36 T. P. I. Hanusa, R. H. Crabtree and D. M. P. Mingos, *Comprsehensive Organometallic Chemistry III*, Elsevier Science, 2007, vol. 2.

37 C. Boone, I. Korobkov and G. Nikonov, *ACS Catal.*, 2013, **3**, 2336–2340.
38 A. Hicken, A. J. P. White and M. R. Crimmin, *Inorg. Chem.*, 2017, **56**, 8669–8682.
39 E. Larionov, H. Li and C. Mazet, *Chem. Commun.*, 2014, **50**, 9816–9826.
40 D. W. Reed, D. R. Polichuk, P. H. Buist, S. J. Ambrose, R. J. Sasata, C. K. Savile, A. R. S. Ross and P. S. Covello, *J. Am. Chem. Soc.*, 2003, **125**, 10635–10640.
41 M. J. Butler, A. J. P. White and M. R. Crimmin, *Angew. Chem., Int. Ed.*, 2016, **55**, 6951–6953.
42 P. Chen, Z. T. Xiong, J. Z. Luo, J. Y. Lin and K. L. Tan, *Nature*, 2002, **420**, 302–304.
43 K. Chłopek, C. Frommen, A. Leon, O. Zabara and M. Fichtner, *J. Mater. Chem.*, 2007, **17**, 3496–3503.
44 C. Wu and H.-M. Cheng, *J. Mater. Chem.*, 2010, **20**, 5390–5400.
45 M. Dornheim, S. Doppiu, G. Barkhordarian, U. Boesenberg, T. Klassen, O. Gutfleisch and R. Bormann, *Scr. Mater.*, 2007, **56**, 841–846.
46 C. M. Stander and R. A. Pacey, *J. Phys. Chem. Solids*, 1978, **39**, 829–832.
47 S. Harder, J. Spielmann, J. Intemann and H. Bandmann, *Angew. Chem., Int. Ed.*, 2011, **50**, 4156–4160.
48 J. Intemann, J. Spielmann, P. Sirsch and S. Harder, *Chem. – Eur. J.*, 2013, **19**, 8478–8489.
49 J. Intemann, P. Sirsch and S. Harder, *Chem. – Eur. J.*, 2014, **20**, 11204–11213.
50 J. Pahl, S. Brand, H. Elsen and S. Harder, *Chem. Commun.*, 2018, **54**, 8685–8688.
51 A. Friedrich, J. Eyselein, J. Langer and S. Harder, *Organometallics*, 2021, **40**, 448–457.
52 A. Friedrich, J. Pahl, H. Elsen and S. Harder, *Dalton Trans.*, 2019, **48**, 5560–5568.
53 H. V. K. Diyabalanage, R. P. Shrestha, T. A. Semelsberger, B. L. Scott, M. E. Bowden, B. L. Davis and A. K. Burrell, *Angew. Chem., Int. Ed.*, 2007, **46**, 8995–8997.
54 Z. Xiong, C. K. Yong, G. Wu, P. Chen, W. Shaw, A. Karkamkar, T. Autrey, M. O. Jones, S. R. Johnson, P. P. Edwards and W. I. F. David, *Nat. Mater.*, 2008, **7**, 138–141.
55 A. Staubitz, A. P. M. Robertson and I. Manners, *Chem. Rev.*, 2010, **110**, 4079–4124.
56 J. Spielmann, D. Piesik, B. Wittkamp, G. Jansen and S. Harder, *Chem. Commun.*, 2009, 3455–3456.
57 S. Harder, J. Spielmann, J. Intemann and H. Bandmann, *Angew. Chem., Int. Ed.*, 2011, **50**, 4156–4160.
58 A. Rit, A. Zanardi, T. P. Spaniol, L. Maron and J. Okuda, *Angew. Chem., Int. Ed.*, 2014, **53**, 13273–13277.
59 A. J. Roberts, W. Clegg, A. R. Kennedy, M. R. Probert, S. D. Robertson and E. Hevia, *Dalton Trans.*, 2015, **44**, 8169–8177.
60 M. Arrowsmith, M. S. Hill, D. J. MacDougall and M. F. Mahon, *Angew. Chem., Int. Ed.*, 2009, **48**, 4013–4016.
61 M. G. Davidson, D. Garcia-Vivo, A. R. Kennedy, R. E. Mulvey and S. D. Robertson, *Chem. – Eur. J.*, 2011, **17**, 3364–3369.
62 D. Mukherjee, H. Osseili, T. P. Spaniol and J. Okuda, *J. Am. Chem. Soc.*, 2016, **138**, 10790–10793.
63 S. Banerjee, Ankur, A. Andrews and A. Venugopal, *Chem. Commun.*, 2018, **54**, 5788–5791.
64 R. Chambenahalli, A. P. Andrews, F. Ritter, J. Okuda and A. Venugopal, *Chem. Commun.*, 2019, **55**, 2054–2057.
65 Ankur, D. Sharma, A. P. Andrews and A. Venugopal, *Dalton Trans.*, 2023, **52**, 1533–1537.
66 R. Chambenahalli, R. M. Bhargav, K. N. McCabe, A. P. Andrews, F. Ritter, J. Okuda, L. Maron and A. Venugopal, *Chem. – Eur. J.*, 2021, **27**, 7391–7401.
67 W. Sattler and G. Parkin, *J. Am. Chem. Soc.*, 2012, **134**, 17462–17465.
68 O. Jacquet, X. Frogneux, C. D. N. Gomes and T. Cantat, *Chem. Sci.*, 2013, **4**, 2127–2131.
69 D. Specklin, C. Fliedel, C. Gourlaouen, J.-C. Bruyere, T. Aviles, C. Boudon, L. Ruhlmann and S. Dagorne, *Chem. – Eur. J.*, 2017, **23**, 5509–5519.
70 M. Rauch and G. Parkin, *J. Am. Chem. Soc.*, 2017, **139**, 18162–18165.
71 K. Ruhlandt-Senge, K. W. Henderson and P. C. Andrews, in *Comprehensive Organometallic Chemistry III*, ed. R. H. Crabtree and D. M. P. Mingos, Elsevier, Oxford, 2007, vol. 2.
72 C. Lichtenberg, J. Engel, T. P. Spaniol, U. Englert, G. Raabe and J. Okuda, *J. Am. Chem. Soc.*, 2012, **134**, 9805–9811.
73 (*a*) K. T. Quisenberry, J. D. Smith, M. Voehler, D. F. Stec, T. P. Hanusa and W. W. Brennessel, *J. Am. Chem. Soc.*, 2005, **127**, 4376–4387; (*b*) S. C. Chmely, C. N. Carlson, T. P. Hanusa and A. L. Rheingold, *J. Am. Chem. Soc.*, 2009, **131**, 6344–6345; (*c*) I. Peckermann, G. Raabe, T. P. Spaniol and J. Okuda, *Chem. Commun.*, 2011, **47**, 5061–5063.
74 Further coordination modes for the allyl ligand were observed for transition metal centres, *e.g.* the interaction of the α- and the γ-positions of an allyl ligand with two metal centres or the interaction with M–M fragments: (*a*) J. B. Sheridan, K. Garrett, G. L. Geoffroy and A. L. Rheingold, *Inorg. Chem.*, 1988, **27**, 3248–3250; (*b*) H. Kurosawa, K. Hirako, S. Natsume, S. Ogoshi, N. Kanehisa, Y. Kai, S. Sakaki and K. Takeuchi, *Organometallics*, 1996, **15**, 2089–2097.
75 C. Lichtenberg and J. Okuda, *Angew. Chem., Int. Ed.*, 2013, **52**, 5228–5246.
76 C. Lichtenberg, T. P. Spaniol, I. Peckermann, T. P. Hanusa and J. Okuda, *J. Am. Chem. Soc.*, 2013, **135**, 811–821.
77 C. Lichtenberg, T. P. Spaniol, L. Perrin, L. Maron and J. Okuda, *Chem. – Eur. J.*, 2012, **18**, 6448–6452.
78 C. Lichtenberg, T. P. Spaniol and J. Okuda, *Angew. Chem., Int. Ed.*, 2012, **51**, 8101–8105.
79 C. Lichtenberg, P. Jochmann, T. P. Spaniol and J. Okuda, *Angew. Chem., Int. Ed.*, 2011, **50**, 5753–5756.
80 E. G. Hoffmann, H. Nehl, H. Lehmkuhl, K. Seevogel and W. Stempfle, *Chem. Ber.*, 1984, **117**, 1364–1377.
81 C. Lichtenberg, T. P. Spaniol, I. Peckermann, T. P. Hanusa and J. Okuda, *J. Am. Chem. Soc.*, 2013, **135**, 811–821.